Journal of Thermal Analysis, Vol. 42 (1994) 1081-1090

NON-ISOTHERMAL DECOMPOSITION OF ANHYDROUS SILVER MALONATE

M. A. Mohamed

Department of Chemistry, Faculty of Science, Qena, Egypt

(Received October 30, 1993; in revised form January 5, 1994)

Abstract

The non-isothermal decomposition of anhydrous disilver malonate was studied up to 300°C by means of TG, DTA and DSC techniques in different atmospheres (e.g. N_2, H_2 and air). Acetic acid, CO_2, acetone and CO were identified as the volatile decomposition products using gas chromatography. Silver metal, on the other hand, was identified as the final solid product using X-ray powder diffraction. The mechanism described involves the breakdown of adsorbed radicals, probably including $-CH_2COO-$ and related species, on the surface of the metallic silver product.

The activation energy (ΔE) and the frequency factor ($\ln A$) were calculated for the decomposition process from the variation of peak temperature (of the DTA curves) with the rate of heating (φ). The enthalpy change (ΔH), the heat capacity (C_p) and entropy change (ΔS) were calculated from the DSC measurements.

Keywords: anhydrous disilver malonate, DTA, DSC, kinetics, TG, X-ray

Introduction

The thermal decomposition of metal malonates has been the subject of several studies [1]. Most of these were concerned with the malonates of transition metals, e.g. cobalt [2], nickel [3] and copper [4, 5].

Galwey and his coworkers carried out [3–8] extensive studies on copper, nickel, silver and calcium malonates. Their work included kinetic, microscopic and mechanistic investigations. The thermal decomposition of copper(II) malonate was reported [4, 5] to proceed through a melt formation and stepwise cation reduction ($Cu^{2+} \rightarrow Cu^{+} \rightarrow Cuo$). Also a reaction intermediate, copper acetate, was found to be formed and subsequently decomposed. Nickel [3] and calcium [6] malonates were found to form the corresponding acetate as a reaction intermediate. NMR technique was used in these studies to monitor the acetate formation and concentration during the decomposition of these salts.

0368–4466/94/ $ 4.00

John Wiley & Sons, Limited
Chichester

Silver malonate, on the other hand, was found [7] to behave differently from the other malonates studied in that it gives acetic acid rather than the acetate produced by the rest of the malonates. Silver metal was the final solid product with a small amount of carbon. The effect of γ-ray on the decomposition of silver malonate was also studied [8]. It was found that pre-irradiation of the salt significantly shortened the induction period prior to the decomposition process.

The present study was undertaken to compare the isothermal kinetic results published earlier [7] with those obtained here by non-isothermal technique. In addition to this, the DSC measurements were used here to calculate some thermodynamic parameters. Another important objective is discussed here concerning the role of hydrogen in the decomposition reaction.

Experimental

Materials and techniques

Anhydrous disilver malonate was prepared by the reaction of silver nitrate with sodium malonate as follows: 17 g of silver nitrate (BDH Chemicals) dissolved in 500 ml deionized water (0.2 mol/l) was added dropwise, with stirring, to 0.1 mol/l solution of sodium malonate (7.4 g sodium malonate, BDH Chemicals, in 500 ml deionized water). A white product of silver malonate was immediately precipitated and was left at 60°C for 6 h with stirring. It was filtered, washed several times with deionized water and was finally dried at 100°C. The reactant salt was kept in a dark bottle to reduce the effect of light.

Thermal analysis, including thermogravimetry (TG), differential thermal analysis (DTA) and differential scanning calorimetry (DSC) was performed using Shimadzu Stand Alone Thermal Analyser Instruments (TGA-50H, DTA-50 and DSC-50), Japan. These instruments were provided with a data processor Chromatopac C-R4AD. The program of the data processor gives the values of temperatures, mass loss and the amount of heat involved in any thermal event.

Experiments were performed in different dynamic atmospheres of N_2, air and H_2 (40 ml/min). TG and DTA curves were recorded on heating up to 300°C at five different heating rates (φ) standardized at 3, 5, 7, 10 and 15 $\text{deg}\cdot\text{min}^{-1}$, while DSC curves were recorded at 5, 7 and 10 $\text{deg}\cdot\text{min}^{-1}$. Constant weights of silver malonate sample (ca. 10–15 mg) were used in order to avoid the effect of variation of sample weight on the peak temperature. Highly sintered α-Al_2O_3 powder (Shimadzu Co.) was used as a reference material for DTA and DSC measurements. The heat of transition (28.24 J/g [9]) of pure indium metal (Johnson Matthey) at 157°C was used for calibration in DSC studies.

X-ray powder diffraction studies on silver malonate and its calcination solid products at some temperatures were carried out by means of a Model JSX-60PA

JEOL diffractometer (Japan) equipped with a source of Ni-filtered CuK_α radiation. Results were matched with ASTM standard cards.

Gas phase decomposition products of anhydrous silver malonate were analysed using a Shimadzu Computerized Gas Chromatograph Model GC-14A, connected with a flow system at atmospheric pressure. Dry N_2 was used as a dynamic atmosphere (85 ml/min) and as a carrier. The analysis was carried out with SUS. Column PEG 6000 10% on Shimalite TPA, 60/80 mesh, 3 mm I.D.x2m at 150°C. Product gases were sensed by a thermal conductivity detector (TCD). Automatic sampling was performed with a Heated Gas sample Cock type HGS-2.

Data analysis

Kinetic parameters such as the activation energy (ΔE, kJ/mol) and the frequency factor ($\ln A$) were calculated for the decomposition process using Kissinger's equation [10]:

$$\frac{\ln \varphi}{T_m^2} = \frac{-\Delta E}{RT} + \ln \frac{AR}{E}$$

where φ is the heating rate (deg·min^{-1}), T_m is the DTA peak temperature and R is the gas constant (8.314 J·mol^{-1}·K^{-1}).

A plot of $\ln\varphi/T^2$ *vs.* $1/T$ gives a straight line, the values of activation energy (ΔE) and the frequency factor ($\ln A$) can be given from the slope and the intercept, respectively.

Thermodynamic parameters namely, the enthalpy change (ΔH), heat capacity (C_p) and the entropy change (ΔS) for each process were calculated from the DSC curves as described elsewhere [11].

Results and discussion

Elemental analysis

Combustion analysis was used for determining hydrogen and carbon and atomic absorption spectrometry for silver. The results obtained were close to the theoretical values of the anhydrous salt $CH_2(COOAg)_2$ (Table 1).

Thermal analysis

Figure 1 shows a TG curve, together with the corresponding DTG curve for the decomposition of silver malonate on heating up to 300°C. The heating rate was 5 deg·min^{-1} in a dynamic atmosphere of N_2 (40 ml/min).

Table 1 Results of elemental analysis for $CH_2(COOAg)_2$

Element	Experimental / %	Theoretical / %
C	11.41	11.34
H	0.69	0.63
Ag	31.98	32.11

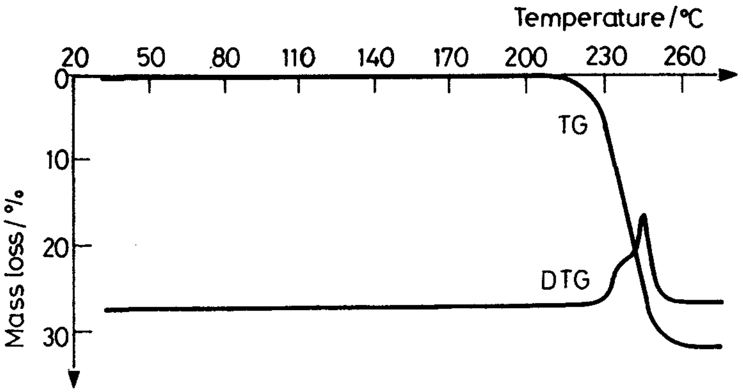

Fig. 1 TG curve recorded in N_2 (40 ml/min) at 5 deg·min^{-1} together with the corresponding DTG curve which shows 2 mass loss maxima

The TG curve shows that anhydrous silver malonate is thermally stable up to 213°C with no mass change. At 213°C, however, the salt starts to lose mass rapidly, reaching a total of 32.06% of the original weight of sample. The DTG curve displays two maxima located at 236.5 and 246.5°C. The appearance of two maxima in the DTG curve was observed for low rates of heating (i.e. 2, 5 and 7 deg·min^{-1}). At higher rates (i.e. 10 and 15 deg·min^{-1}) only one maximum appeared (Table 2). It should be pointed out here that at high rates of heating (≥15 deg·min^{-1}) the measurements were not reliable, because some of the reac-

Table 2 Summary of TG and DTG results

Heating rate / deg·min^{-1}	Total mass loss / %	T_{max} (1) / °C	T_{max} (2) / °C
3	31.98	223.1	231.9
5	32.06	236.5	246.5
7	32.15	241.3	249.6
10	32.07	–	253.8
15	36.78	–	256.2

tant sample was sputtered out of the pan as a result of the vigorous evolution of volatile gaseous products. This, in turn, has resulted in an apparent increase in the total mass loss (Table 2).

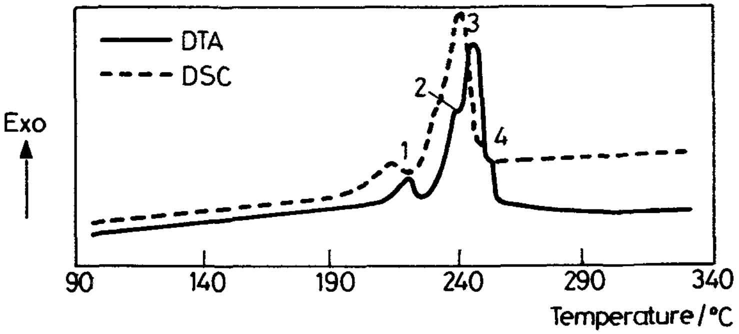

Fig. 2 DTA and DSC curves recorded at 5 deg·min^{-1} in a dynamic atmosphere of N_2 (40 ml/min)

Figure 2 shows a DTA curve together with a DSC curve, both taken at 5 deg·min^{-1} under a dynamic atmosphere of N_2 (40 ml/min). The DTA curve displays four exothermic peaks. The first is located at 219.7°C which is followed by three overlapped exothermic peaks located at 238.3, 245 and 252.5°C respectively. The effect of variation of heating rate on the peak temperature is shown in Table 3.

Table 3 Summary of DTA results

Heating rate /	T_{max} / °C			
deg·min^{-1}	Exo (1)	Exo (2)	Exo (3)	Exo (4)
3	210.0	230.7	239.8	244.0
5	219.7	238.3	245.0	252.5
7	–	242.5	251.6	–
10	–	247.5	257.0	261.4

The activation energy (ΔE kJ/mol) and the frequency factor ($\ln A$) of the decomposition process were calculated from the DTA data (shown in Table 3) for peaks 2, 3 and 4; peak 1 was excluded since there were two values only. Values of ΔE, $\ln A$ and the correlation coefficients are listed in Table 4. It is clear that the values of ΔE as well as $\ln A$ are relatively close for the 3 processes.

The DSC curve (Fig. 2) is similar to the DTA curve since it displays 4 exothermic peaks. The first small peak is located at 213°C which is followed by two

Table 4 Kinetic parameters of the decomposition of silver malonate

Parameter	Peak (2)	Peak (3)	Peak (4)
ΔE / kJ·mol^{-1}	148.98	144.11	150.55
ln A	33.99	32.22	33.40
Correlation coeff.	0.999	0.990	0.997

overlapped exothermic peaks at 231 and 241°C, the last exothermic process appears as a small shoulder at 251°C. The enthalpy change of the decomposition (ΔH), the heat capacity (C_p) and the entropy change (ΔS) were calculated using peaks 2 and 3. The values of these parameters are listed in Table 5. It should be stated here that process 1 (peak 1) in Table 5 refers to the decomposition of silver malonate to form silver oxide or silver carbonate intermediates. Process 2 (peaks 2–4), on the other hand, refers to the main catalytic decomposition of the adsorbed radicals on the silver metal surface.

Table 5 Thermodynamic parameters of the decomposition reaction

Parameter	In nitrogen		In hydrogen	
	process 1	process 2	process 1	process 2
ΔH / kJ·mol^{-1}	2.0	118	–	58.91
C_p / J·g^{-1}·deg^{-1}	0.46	1.09	–	0.46
ΔS / J·g^{-1}·deg^{-1}	0.04	0.99	–	0.26

Effect of the atmosphere

Three TG experiments were carried out at the same heating rate (ca. 5 deg·min^{-1}) and with equal weights of sample (12 mg). The only difference was in the applied dynamic atmosphere where N_2 was used in one experiment, dry air in the second and H_2 was used in the third experiment (with the same rate of flow, 40 ml/min). The results are displayed in Fig. 3. The use of N_2 or dry air atmospheres have resulted in two similar TG curves where the temperature at which the decomposition started was measured as 213°C (in N_2) and 214.5°C (in air). In addition, the DTG curves of both experiments were closely similar in that each curve showed two maxima, i.e. at 236.5 and 246.5°C (for N_2) and at 235 and 243.5°C (in an atmosphere of air).

In H_2 atmosphere, on the other hand, the decomposition temperature was shifted to a much lower value (ca. 176.3°C). Also, the DTG curve showed a single maximum located at 230.7°C (instead of two maxima in N_2 or in air).

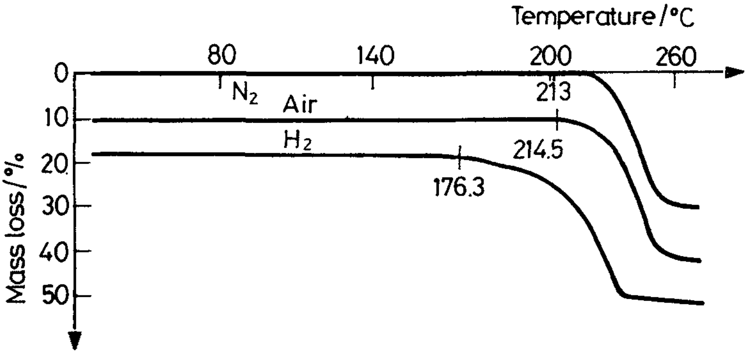

Fig. 3 The effect of the atmosphere on the decomposition of silver malonate. All three TG curves were recorded at 5 deg·min^{-1} in different atmospheres of N_2, air and H_2

The effect of hydrogen is also shown in Fig. 4, where two DSC curves are presented which were taken at the same heating rate (ca. 5 deg·min^{-1}) using an equal weight of sample (ca. 10 mg). N_2 was used as a dynamic atmosphere in one experiment and H_2 for the other (both were performed at a flow rate of 40 ml/min). Again, in H_2 atmosphere the first small exothermic peak disappeared while the main exothermic peak was shifted to a lower temperature of 234°C (compared to 241°C in the presence of N_2 atmosphere).

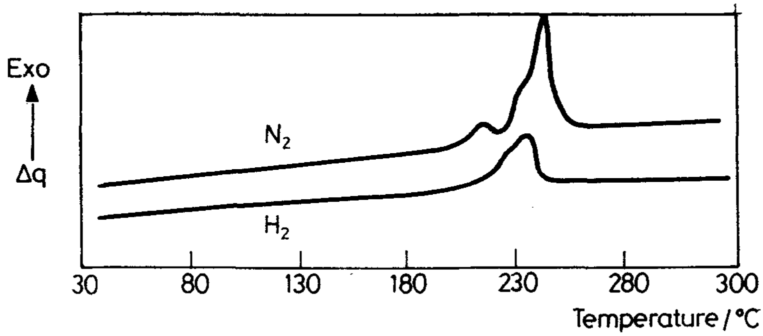

Fig. 4 Two DSC curves taken at 5 deg·min^{-1}, one taken in N_2 while the other in H_2 atmosphere

The enthalpy change (Δ*H*), heat capacity (C_p) and entropy change (Δ*S*) of the decomposition of silver malonate in H_2 were calculated from the DSC curve (Fig. 4). In hydrogen atmosphere, however, the values of these thermodynamic parameters were reduced to almost half of the values measured in an atmosphere of N_2 (Table 5).

X-ray diffraction method was used to identify the solid reaction intermediates which may, possibly, participate in the decomposition of silver malonate.

For this purpose, a number of samples were heated in an atmosphere of N_2 for 60 min (between 210–220°C). These samples were subjected to X-ray analysis. The results obtained did not reveal any intermediate formation. This is, possibly, due to the fact that the decomposition proceeds very rapidly and gets completed in less than 2 or 3 minutes. The X-ray diffractogram of the solid product gave a pattern that matched well the pattern of silver metal (ASTM card 4-783).

Gas chromatography

The volatile decomposition products were identified using gas chromatography. Figure 5 shows the distribution of these products of heating of silver malonate at 210°C in N_2 atmosphere (at 85 ml/min). Acetic acid represents the major product with 81% of the total yield and CO_2 is the second major product (13.5% of the product). Acetone and CO gas were also produced. Their proportions represented 3.7% and 0.4% of the total yield, respectively.

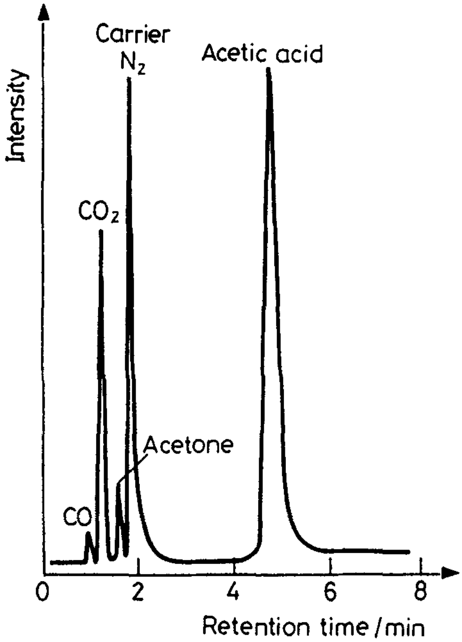

Fig. 5 GC analysis of the volatile decomposition products obtained by heating silver malonate at 210°C in a dynamic atmosphere of N_2

Reaction mechanism

There is a similarity between the results of the present work and the information available [12, 13] about the decomposition of silver acetate which proceeds in comparable temperature intervals. Also, the similarity extends to the decomposition products (CO_2, CH_3COOH, carbon and silver metal). This leads to the conclusion that the controlling steps at the reaction interface during silver malonate decomposition could be the same as those participating in the reaction of acetate ions adsorbed on metallic silver [14]. Hence, surface equilibria are expected to set up between the adsorbed radicals which we have previously detected by ESR measurements, and probably the same controlling parameters in product desorption. Silver metal was shown [7] to have a promoting effect on the decomposition of silver malonate. This could be due to the fact [15] that hydrogen transfer becomes appreciable at the reaction temperature, thus permitting reorganization of the chemisorbed $-CH_2COO-$ groups. This agrees well with the observed promoting effect of hydrogen in the present study.

The possible participation of solid intermediates e.g. Ag_2CO_3 or Ag_2O as precursor for the silver metal formation could not be proved experimentally because the decomposition was very fast. Also, both compounds are known [9] to decompose at 218 and 230°C (i.e. within the temperature range at which the reaction becomes too fast to permit the detection of intermediates.

The observed enhancing effect of H_2 on the decomposition of silver malonate can be explained by the fact that it provides a reducing atmosphere for Ag_2CO_3 or Ag_2O to form silver metal which acts as the active surface for the autocatalytic decomposition.

Finally, it is worth mentioning here that the values of ΔE and $\ln A$, obtained here, agree well with those calculated earlier from an isothermal study [7] where ΔE was reported as 161 kJ/mol (compared to 150.5 kJ/mol here) and $\ln A$ was reported as 33 (compared to 33.9 and 33.4 in the present study).

References

1 M. E. Brown, D. Dollimore and A. K. Galwey, Reactions in the Solid State, Comprehensive Chemical Kinetics, vol. 22 Elsevier, Amsterdam 1980.

2 A. K. Galwey, D. M. Gamieson, M. Le Van and C. Berro, Thermochim. Acta, 10 (1974) 161.

3 A. K. Galwey, S. G. McKee, T. R. B. Mitchell, M. A. Mohamed, M. E. Brown and A. F. Bean, Reactivity of Solids, 6 (1988) 187.

4 N. J. Carr and A. K. Galwey, Proc. R. Soc. London A, 404 (1986) 101.

5 N. J. Carr, A. K. Galwey and M. A. Mohamed, Thermochim. Acta, 102 (1986) 323.

6 A. K. Galwey and M. A. Mohamed, Solid State Ionics, 42 (1990) 135.

7 A. K. Galwey and M. A. Mohamed, J. Chem. Soc., Faraday Trans. I, 81 (1985) 2503.

8 A. K. Galwey, P. J. Herley and M. A. Mohamed, J. Chem. Soc., Faraday Trans. I, 84 (1988) 729.

9 R. C. Weast (Ed.), Handbook of Chemistry and Physics (62nd edn.) CRC Press, New York 1982.

10 H. E. Kissinger, J. Anal. Chem., 29 (1957) 1702.

11 M. A. Mohamed and S. A. Halawy, J. Thermal Anal., 41 (1993) 147.

12 M. D. Judd, B. A. Plunkett and M. I. Pope, J. Thermal Anal., 6 (1974) 555.
13 P. Baraldi, Spectrochim. Acta, 38A (1982) 51.
14 M. A. Barteau, M. Bowker and R. J. Madix, J. Catal., 67 (1981) 118.
15 C. Kemball and C. T. H. Stoddart, Proc. R. Soc. London, Ser. A, 241 (1957) 208.

Zusammenfassung — Mittels TG, DTA und DSC wurde in verschiedenen Atmosphären (Stickstoff, Wasserstoff, Luft) bis 300°C die nichtisotherme Zersetzung von wasserfreiem Disilbermalonat untersucht. Mittels Gaschromatographie konnten als flüchtige Zersetzungsprodukte Essigsäure, CO_2, Aceton und CO festgestellt werden. Anhand von Pulver-Röntgenaufnahmen konnte auf der anderen Seite Silber als festes Endprodukt identifiziert werden. Der beschriebene Mechanismus beinhaltet den Zerfall von adsorbierten Radikalen, die wahrscheinlich $-CH_2COO-$ und verwandte Spezies enthalten, an der Oberfläche des metallischen Silberproduktes.
Die Aktivierungsenergie (ΔE) und der Frequenzfaktor ($\ln A$) für den Zersetzungsprozeß wurden anhand der Änderung der Peaktemperatur (der DTA-Kurven) in Abhängigkeit von der Aufheizgeschwindigkeit φ berechnet. Die Enthalpie (ΔH), Wärmekapazität (C_p) und die Entropieänderung (ΔS) wurden anhand der DSC-Messungen errechnet.